Origin of the Glomerular Basement Membrane Visualized after In Vivo Labeling of Laminin in Newborn Rat Kidneys

DALE R. ABRAHAMSON
Department of Cell Biology and Anatomy, University of Alabama at Birmingham, Birmingham, Alabama 35294

ABSTRACT To examine the origin and assembly of glomerular basement membranes (GBMs), affinity purified anti-laminin IgG was directly coupled to horseradish peroxidase (HRP) and intravenously injected into newborn rats. Kidneys were then processed for peroxidase histochemistry and microscopy. Within 1 h after injection, anti-laminin bound to basement membranes of nephrons in all developmental stages (vesicle, comma, S-shaped, developing capillary loop, and maturing glomeruli). In S-shaped and capillary loop glomeruli, anti-laminin-HRP labeled a double basal lamina between the endothelium and epithelium. Sections incubated with anti-laminin in vitro showed labeling within the rough endoplasmic reticulum of endothelium and epithelium, indicating that both cell types synthesized laminin for the double basement membrane. In maturing glomeruli, injected anti-laminin-HRP bound throughout the GBMs, and double basement membranes were rarely observed. At this stage, however, numerous knobs or outpockets of basement membrane material extending far into the epithelial side of the capillary wall were identified and these were also labeled throughout their full thickness. No such outpockets were found in the endothelial cell layer of newborn rats (and they normally are completely absent in fully mature, adult glomeruli). In contrast with these results, in kidneys fixed 4–6 d after anti-laminin IgG-HRP injection, basement membranes of vesicle, comma, and S-shaped nephrons were unlabeled, indicating that they were assembled after injection. GBM labeling was seen in maturing glomeruli, however. In addition, the outpockets of basement membrane extending into the epithelium were often completely unlabeled whereas GBMs lying immediately beneath them were labeled intensely, which indicates that the outpockets were probably assembled by the epithelium. Injections of sheep anti-laminin IgG followed 8 d later with injections of biotin-rabbit anti-laminin IgG and double-label immunofluorescence microscopy confirmed that GBM formation continued during individual capillary loop expansion. GBM assembly therefore occurs by at least two different processes at separate times in development: (*a*) fusion of endothelial and epithelial basement membranes followed by (*b*) addition of new basement membrane from the epithelium into existing GBMs.

The glomerular basement membrane (GBM)[1] constitutes the principal filter for plasma macromolecules in the kidney (10; reviewed in references 18 and 26). In addition, the GBM is unusual in that it serves as a common basement membrane shared by two different cell types: the fenestrated endothelium, which lines the glomerular capillaries, and the extensively interdigitated visceral epithelium, or podocytes, which face the urinary space. Indeed, a commonly held belief is that the GBM arises during development from the fusion of endothelial and epithelial basement membranes (27, 42, 46, 47, 50). As is the case with other basement membranes, the GBM contains type IV collagen (28), heparan sulfate, and chondroitin sulfate proteoglycans (23, 24, 34), and the glycopro-

[1] *Abbreviations used in this paper:* GBM, glomerular basement membrane; HRP, horseradish peroxidase; TBM, tubular basement membrane.

THE JOURNAL OF CELL BIOLOGY · VOLUME 100 JUNE 1985 1988-2000

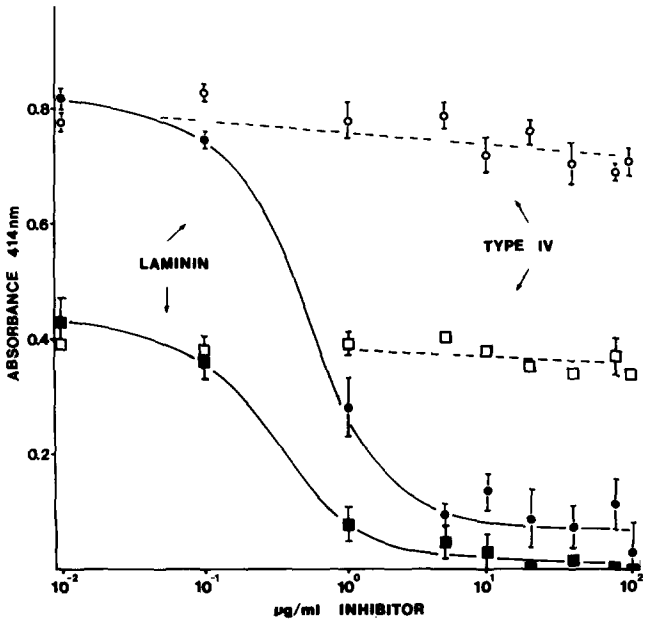

FIGURE 1 Plot of data from inhibition enzyme-linked immunosorbent assay. Microtiter wells were coated overnight with 50 µl of a solution of 20 µg/ml laminin and then washed and blocked with 10% horse serum. 50-µl aliquots of ~0.8 µg/ml rabbit anti-laminin IgG were preincubated overnight with 0.01–100 µg/ml of laminin (—●—) or type IV collagen (- - -○- - -) and then added to the laminin-coated plates. Similarly, sheep anti-laminin IgG was preincubated with laminin (—■—) or type IV collagen (- - -□- - -) before plating on laminin. Lines above and below the points represent the standard error of the mean from triplicate assays. Note that laminin, but not type IV collagen, inhibits anti-laminin IgG binding.

teins entactin (9), nidogen (49), and laminin (48). The ultrastructural distribution of laminin within the mature GBM of adult rats has previously been investigated by the intravenous injection of affinity purified anti-laminin IgG coupled directly to horseradish peroxidase (HRP) (1–3). These results, and those of others who used in vitro applications of anti-laminin IgG and indirect immunocytochemistry (32, 33, 36–38), indicated that laminin is present throughout the full thickness of basement membranes. Precisely how laminin and the other large, elongated basement membrane macromolecules are oriented within the GBM and how the GBM is assembled is uncertain, however.

The newborn rat kidney presents a unique opportunity for examining basement membrane assembly because it contains glomeruli in all stages of development. Embryonic glomeruli are found beneath the renal capsule in the outer cortex whereas essentially mature glomeruli are present in the juxtamedullary area (13). Under inductive influences from branching uretic buds (14–16), new glomeruli continue to develop during cortical expansion until ~2 wk after birth (13). In addition, previous immunofluorescence studies of fetal and neonatal mouse kidneys have localized laminin in basement membranes of nephrons from their earliest stages of morphogenesis (14–16). In the experiments described here, I labeled developing renal basement membranes in vivo by intravenously injecting anti-laminin IgG into newborn rats. I then traced the labeled basement membranes by immunofluorescence and immunoelectron microscopy over time as development proceeded.

MATERIALS AND METHODS

Animals: Sprague-Dawley rats in late-term pregnancy were obtained from Southern Animal Farms (Prattville, AL). For the purpose of newborn rat aging, day 1 was considered to be the day of birth.

Proteins and Reagents: Laminin was purified from the Englebreth-Holm-Swarm murine sarcoma by a modification of the method of Timpl et al. (48) as previously described (1). The electrophoretic behavior (1, 3) and amino acid composition (1) of this laminin was nearly identical to that originally reported by Timpl et al. (48), but distinctly different from that of entactin (9) or nidogen (49). In addition, a uronic acid assay (7) showed the absence of detectable hyaluronic acid in this laminin preparation (sensitivity of assay ~1 µg/ml). Affinity-purified sheep and rabbit anti-laminin IgG were eluted from columns of laminin-Sepharose as before (1–3) and, as shown previously by others (48), did not cross-react with purified fibronectin (1). The affinity purified IgGs were also tested for possible cross-reactivity with mouse type IV collagen (kindly provided by Dr. Richard Mayne of this department) in an inhibition enzyme-linked immunosorbent assay. 50-µl aliquots of 0.8 µg/ml anti-laminin IgG were preincubated for 12–18 h with either laminin or type IV collagen ranging in concentration from 0.01–100 µg/ml, and then incubated on laminin-coated microtiter plates. Laminin, but not type IV collagen, inhibited the binding of anti-laminin to the plates (Fig. 1). The sheep and rabbit IgG that failed to bind to laminin-Sepharose were used as laminin-adsorbed IgGs in control experiments.

Affinity purified sheep and rabbit anti-laminin IgG, and laminin-adsorbed IgGs, were conjugated directly to activated HRP (Type VI; Sigma Chemical Co., St. Louis, MO) (39). Rabbit anti-laminin and laminin-adsorbed IgGs were also conjugated to the *N*-hydroxysuccinimide ester of biotin (Miles Scientific Div., Miles Laboratories, Inc., Naperville, IL) (5).

Fluorescein-anti-sheep and anti-rabbit IgGs were obtained commercially (Cooper Biomedical Inc., Malvern, PA). Rhodamine-conjugated avidin was purchased from Vector Laboratories Inc. (Burlingame, CA).

TABLE I

Age and Number of Rats Examined after In Vivo Labeling of Kidney Basement Membranes

Procedure	Age of rat*
Immunoperoxidase light and electron microscopy	
Pulse with anti-laminin IgG-HRP, fix 1 h later	2 (3), 5 (1)
Pulse with control IgG-HRP-fix	2 (1), 5 (1)
Pulse with anti-laminin-HRP-2 d chase-fix	2 (3)
Pulse-3 d chase-fix	3 (2)
Pulse-4 d chase-fix	4 (3)
Pulse-5 d chase-fix	2 (2)
Pulse-6 d chase-fix	2 (2)
Postfixation labeling with anti-laminin-HRP	2 (1), 7 (1)
Postfixation labeling with control IgG-HRP	2 (1)
Standard electron microscopy	2 (2), 4 (1), 5 (1)
Immunofluorescence microscopy	
Pulse with sheep anti-laminin IgG, examine 1 h later	2 (2)
Pulse with control IgG	2 (2)
Pulse with sheep anti-laminin-2 d chase-pulse with biotin-rabbit anti-laminin, examine 1 h later	2 (2), 8 (2)‡
Pulse-3 d chase-pulse	3 (3)
Pulse-7 d chase-pulse	2 (3), 3 (1)
Pulse-8 d chase-pulse	4 (3)
Pulse with control IgG-biotin	2 (2)

* Age in days after birth. Day 1 was considered to be the day of birth. (Numbers in parentheses refer to the number of animals examined at each age.)

‡ In pulse-chase-pulse experiments, the age shown was the age at the time of the first injection.

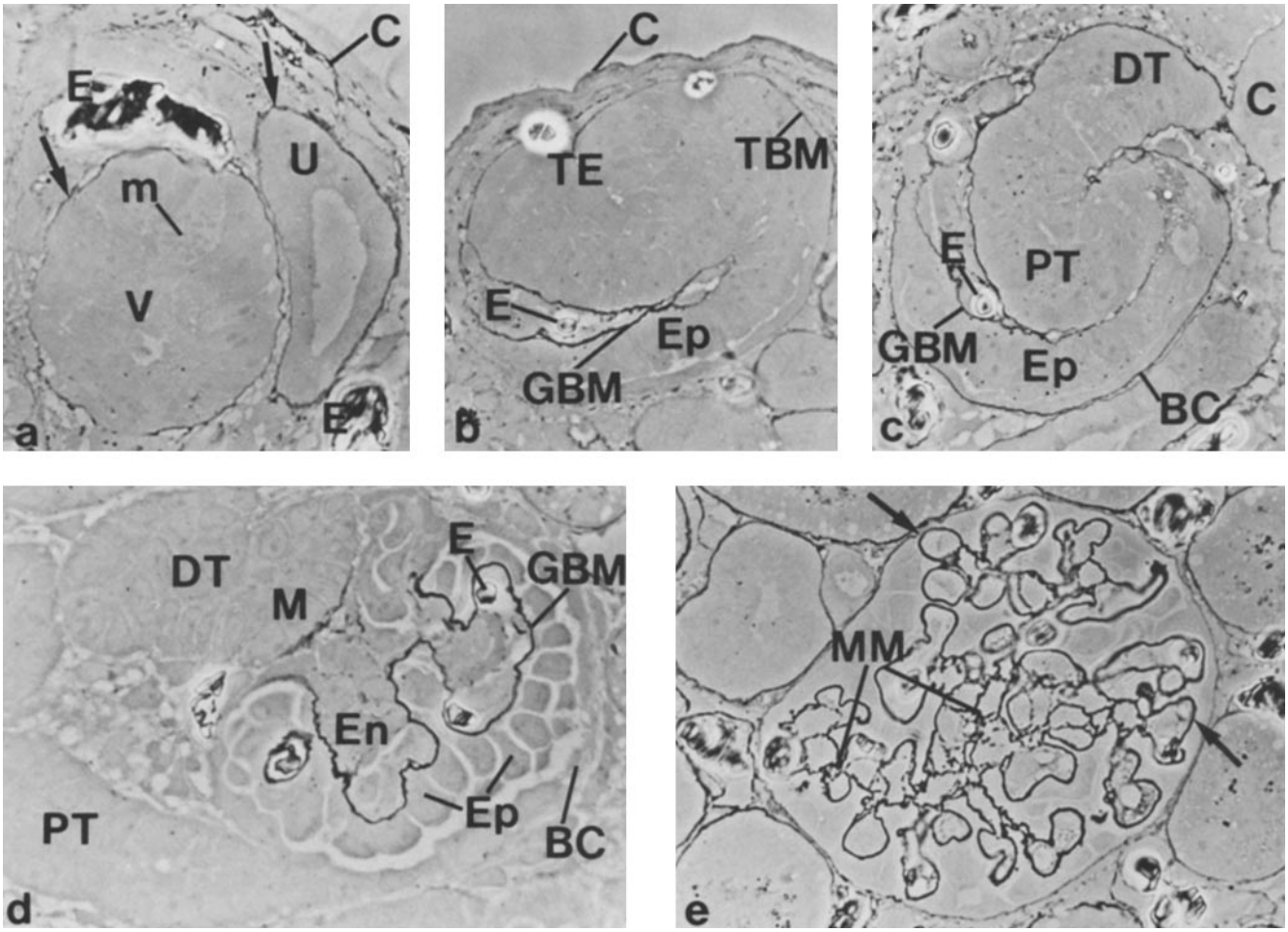

FIGURE 2 Phase-contrast photomicrographs of 0.5–1.0-μm-thick plastic sections of newborn rat developing nephrons after the intravenous injection of anti-laminin IgG-HRP and fixation 1 h later (pulse-fixed). (*a*) The first stage in nephrogenesis occurs just beneath the renal capsule (*C*). Terminal ampulla of the uretic bud (*U*) induce the formation of a vesicle (*V*) of mesenchymal cells. Mitotic figures (*m*) are present within the body of the vesicle. Both the vesicle and uretic bud are surrounded by a peroxidase-positive basement membrane (arrows). *E*, erythrocytes. × 850. (*b*) After vesicle formation, a cleft carrying mesenchymal cells and erythrocytes (*E*) invaginates the primitive nephron. Cells lying beneath the cleft will eventually develop into epithelial (*Ep*) podocytes and are attached to the developing GBM. Those lying above the cleft will develop into tubular epithelium (TE) and some of these are attached to TBM. *Ep*, glomerular epithelium. × 750. (*c*) The next, S-shaped stage occurs as a second cleft develops above the first. The developing nephron can now be subdivided into glomerular region with GBM, gomerular epithelium (*Ep*), and Bowman's capsule (*BC*); proximal tubule (*PT*); and distal tubule (*DT*). *E*, erythrocytes. Note that an apparently continuous basement membrane surrounds these structures and is now also continuous with that of the collecting system (*C*). × 800. (*d*) Capillary loop stage. Here the vascular pole of the forming glomerulus contains endothelial (*En*) and probably mesangial cells. A few erythrocytes (*E*) within glomerular capillaries can be seen. The developing GBM completely envelopes the invading endothelium. Lying outside the GBM are the visceral epithelial podocytes (*Ep*) and the parietal epithelium that lines Bowman's capsule (*BC*). Anlage of the proximal tubule (*PT*) and distal tubule (*DT*) are also present within this section. Although here the TBMs are largely unstained, this rat received a lower injected dose of anti-laminin IgG-HRP than those pictured in Fig. 2, *a–c* and *e* (0.2 vs. 0.3 ml). Note, however, that the basement membrane beneath what probably will become the macula densa (*M*) is stained. × 950. (*e*) Glomerulus in the maturing stage. The structure now resembles fully mature glomeruli but here has attained only ~40% of its final size. Anti-laminin HRP binds to the GBM in peripheral capillary loops (arrows) and throughout the mesangial matrix (*MM*). × 725.

Experimental Procedures: 2–8 d after birth, newborn rat pups were anesthetized with ether and the saphenous vein was exposed. Rats then received intravenous injections via a 30-ga needle of 0.2–0.3 ml of anti-laminin IgG, anti-laminin IgG-HRP, or control IgGs (1.0 mg IgG/ml, 0.3 mg HRP/ml). For pulse-fix labeling studies, IgG-HRP was injected and 1 h later kidneys were fixed in situ and processed as described below. For pulse-chase-fix studies, the injected pups were allowed to recover from the anesthetic and then were returned to the litter. From 2 to 6 d thereafter, rats were re-anesthetized and the left kidney was fixed in situ and removed. In pulse-chase-pulse experiments, newborns that had received sheep anti-laminin IgG 2 d after birth were injected a second time, 3–8 d after birth, with 0.2–0.4 ml of biotin-conjugated rabbit anti-laminin IgG (1.0 mg IgG/ml). The left kidney was removed 1 h after the second injection. The age and number of rats in each set of experiments are shown in Table I.

Microscopy: For immunofluorescence, 4–6-μm-thick cryostat sections of unfixed kidneys were air-dried and then incubated with fluorochrome-conjugated anti-sheep or anti-rabbit IgGs. In pulse-chase-pulse kidneys, the sections were doubly labeled with fluorescein-rabbit anti-sheep IgG and rhodamine-avidin and examined by epifluorescence.

For immunoperoxidase, kidneys from IgG-HRP injected rats were fixed in situ by the subcapsular injection (10) of 2% glutaraldehyde in 0.1 M phosphate buffer, pH 7.3. Pie-shaped sections of fixed cortex, 30–40 μm thick, were then obtained with a Vibratome (Ted Pella, Inc., Irvine, CA) by cutting perpendicular to the capsule. Sections were incubated in 0.01% H_2O_2 and 0.05% diaminoben-

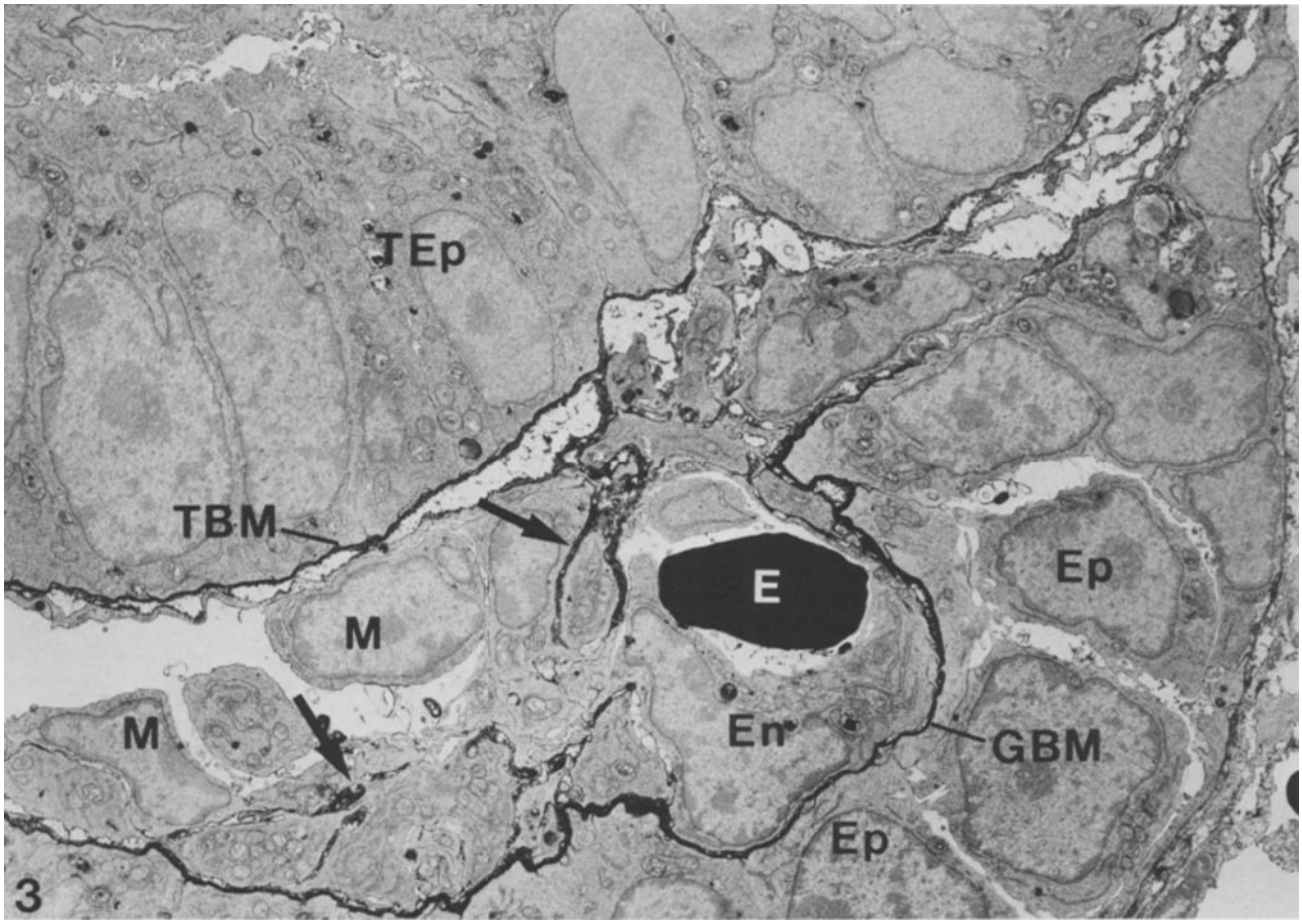

FIGURE 3 Electron micrograph of the lower cleft region of an S-shaped stage nephron from a rat pulse-fixed with anti-laminin IgG-HRP. An erythrocyte (*E*) is densely stained due to the peroxidatic activity of hemoglobin. HRP is present throughout the full thickness of the developing GBM separating the endothelium (*En*) and primitive glomerular epithelium (*Ep*). Some strands of basement membrane-like material lie within the cleft (arrows) between mesenchymal cells (*M*). HRP is also present throughout the full thickness of the TBM underlying the tubular epithelium (*TEp*). × 4,160.

zidine (20) at pH 6.0 (44) and postfixed for 2 h in 2% OsO_4 in 0.1 M phosphate. Tissue was then flat-embedded in upside-down hinged capsules. By this procedure, microtome sections of cortex extending from the capsule to the juxtamedullary zone could readily be obtained. Unstained semithin sections, 0.5–1.0 μm thick, were examined by phase-contrast microscopy. Ultrathin sections, ~70 nm thick, were stained for 1 min in lead citrate (43).

For postfixation immunoperoxidase localization studies, kidneys from 2-d-old uninjected rats were fixed with 4% paraformaldehyde in 0.1 M phosphate, pH 7.3, for 2 h and then washed overnight in buffer. Wedges of fixed cortex were equilibrated for 1 h in 15% sucrose in buffer and frozen on a block of dry ice. 30–40 μm-thick frozen sections were obtained with a sliding microtome (Reichert Scientific Instruments, Buffalo, NY) and then treated for 1 h at room temperature with 0.5% sodium borohydride (35) to inactivate excess aldehydes introduced into the tissue by the fixative. Sections were incubated for 1 h more with 1.0 mg/ml bovine serum albumin in buffer, washed, and then incubated overnight with 25 μg/ml rabbit anti-laminin IgG-HRP or laminin-adsorbed IgG-HRP. Sections were then extensively washed, refixed with 2% glutaraldehyde for 15 min, and processed for peroxidase histochemistry and electron microscopy as described above.

For standard electron microscopic examination, kidneys from uninjected newborn rats were fixed in situ by the subcapsular injection (10) of 1.6% paraformaldehyde and 3% glutaraldehyde in 0.1 M sodium cacodylate, pH 7.4 (25). Cubes of cortex were postfixed in 1% OsO_4 in veronal-acetate, stained en bloc with uranyl acetate (17), and embedded. Thin sections were doubly stained with uranyl acetate and lead citrate (43).

Morphometry: Capillary loop GBM measurements were made as follows. 8 × 10-in prints of electron micrographs of maturing but otherwise randomly selected neonatal glomeruli were placed on a Hipad digitizing tablet (Houston Instruments, Austin, TX) interfaced with an Apple IIplus microcomputer (Apple Computer Inc., Cupertino, CA). By use of a Bioquant II Digitizing Morphometry program (R & M Biometrics Inc., Nashville, TN), lengths of peripheral capillary loop GBM beginning and ending at the endothelial-mesangial border were traced onto the digitizer with a crosshair cursor, measured, and statistically analyzed.

RESULTS

Pulse–Fix Labeling Studies of Developing GBMs

Several authors have described sequential stages in the development of the nephron (13, 15, 22, 27, 41, 42, 47, 50). With the intravenous injection of anti-laminin-HRP into newborn rats, the basement membranes of nephrons at all stages of development (vesicle, comma, S-shaped, developing capillary loop, and maturing glomeruli) were labeled in vivo and could be readily visualized (Fig. 2).

Electron microscopy of S-shaped nephrons showed the peroxidase-labeled basement membranes of the primitive glomerulus (Fig. 3). The basement membranes surrounding the endothelia of nascent blood vessels were in close contact with sheets of cuboidal cells in the process of developing into the glomerular epithelium. The epithelial foot processes typical in adult glomeruli were absent at this early stage. Anti-laminin-HRP was also present throughout the full thickness of the basement membrane beneath the developing tubular epithelium (Fig. 3).

During capillary loop formation, the glomerular epithelium

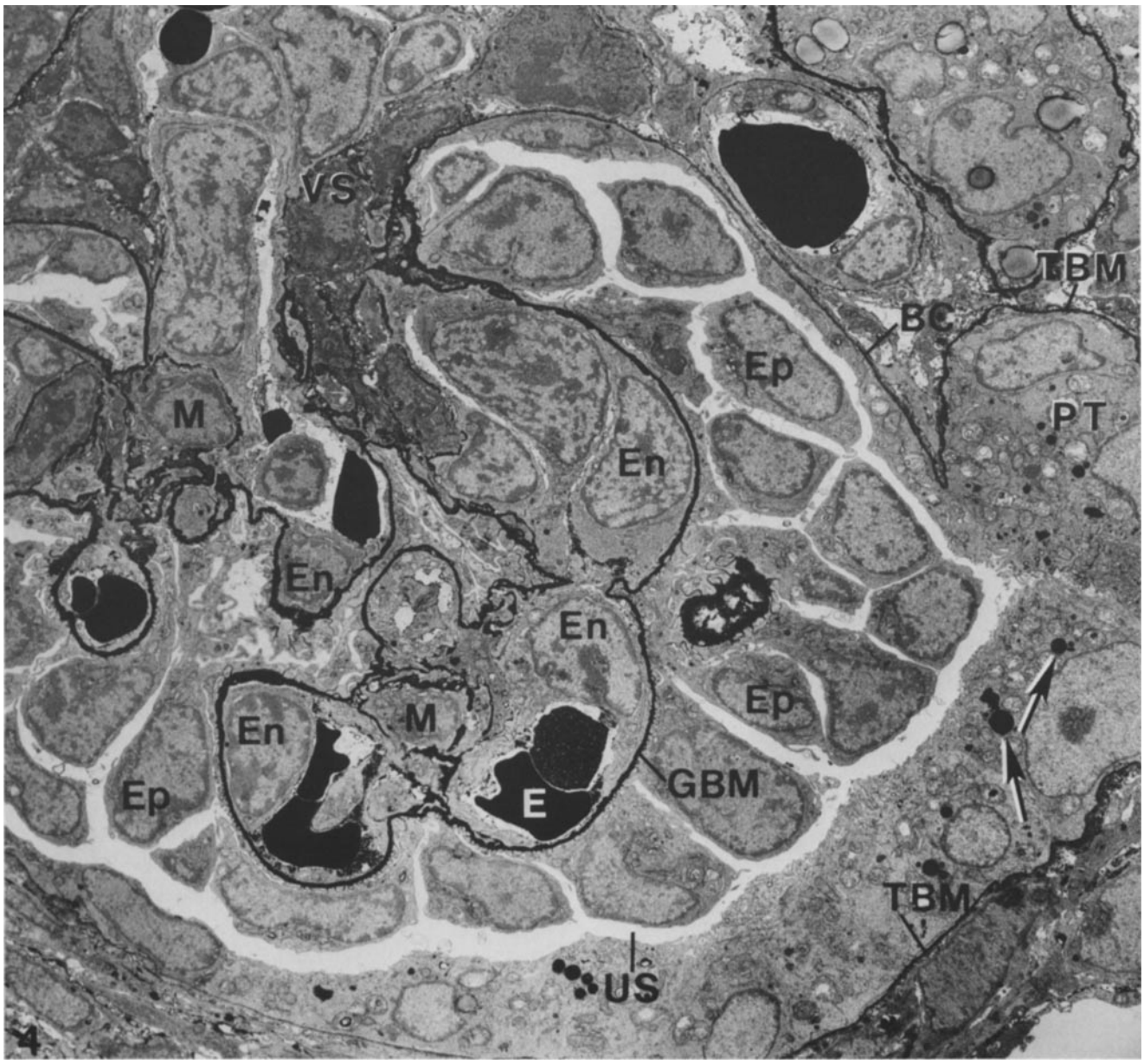

FIGURE 4 Capillary loop stage glomerulus from a newborn pulse-fixed rat. Erythrocytes (*E*) endothelial (*En*) and mesangial (*M*) cells can now be identified within capillary loops. Note that the GBM is stained throughout the capillary loops and is continuous with the basement membranes of the vascular stalk (*VS*) at the top of the figure, Bowman's capsule (*BC*) to the right, and with the TBM that underlies the proximal tubule (*PT*). The transition between the squamous epithelial cells lining Bowman's capsule to the microvilli-studded cells of the proximal tubule is also evident. In addition to basement membranes, HRP is also present within vesicles and dense bodies within the cytoplasm of the proximal tubular epithelium (arrows). *Ep*, glomerular epithelium; *US*, urinary space. × 3,150.

adhering to the developing GBM continues to differentiate and begin foot process formation. In nephrons at this stage (Fig. 4), anti-laminin-HRP was present throughout the full thickness of the GBM in peripheral capillary loops. The basement membrane was also seen to run continuously from capillary loops to the vascular stalk of glomeruli, around Bowman's capsule, and then beneath the epithelium of the proximal tubule (Fig. 4). In addition to completely labeling all basement membranes, peroxidase reaction product was present intracellularly within apical endocytic vesicles and dense bodies of the tubular epithelial cells (Fig. 4).

When the developing GBMs in the S-shaped and developing capillary loop stage glomeruli were examined at higher magnification, a double basement membrane (one beneath the endothelium and one beneath the epithelium) was often observed (Fig. 5). In rats pulse-labeled with anti-laminin-HRP, reaction product always intensely decorated both layers of the double basement membranes (Fig. 5*a*). To determine the origin of this double basement membrane, lightly fixed sections of cortex from uninjected rats were incubated in vitro with anti-laminin IgG-HRP. In addition to the double basement membrane, anti-laminin was present within the rough

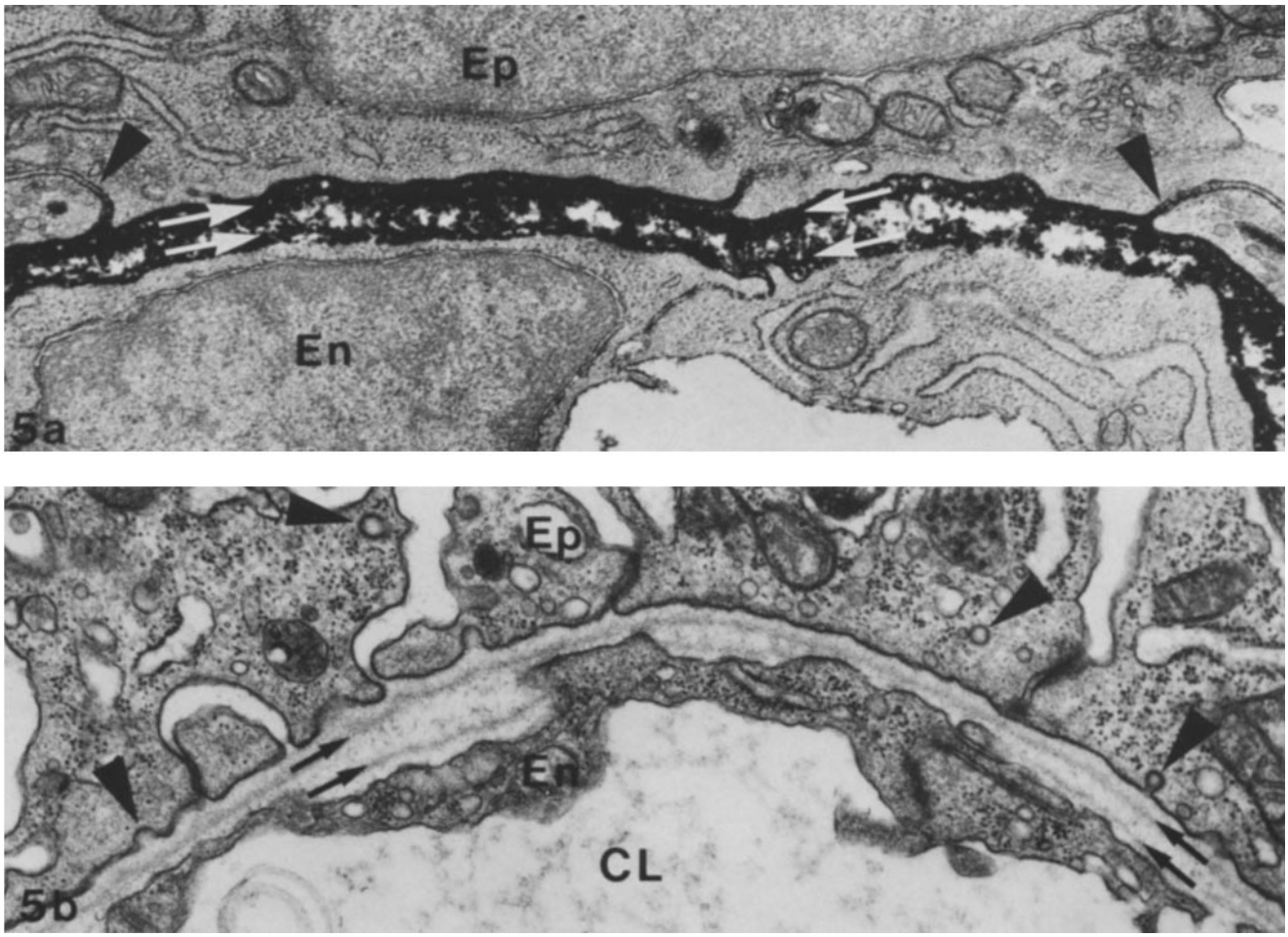

FIGURE 5 Higher magnification views of the glomerular capillary wall in capillary loop stage glomeruli from (*a*) rats pulse-fixed with anti-laminin IgG-HRP and (*b*) normal uninjected rats processed for standard electron microscopy. In *a* a double layer of peroxidase-positive basement membrane-like material (white arrows) is seen between the endothelium (*En*) and epithelium (*Ep*). Epithelial foot processes are poorly developed at this stage, and broad areas of the basal epithelial plasma membrane are adhering to the epithelial basement membrane. Developing epithelial slit diaphragms appear as ladder-like structures (arrowheads), as shown previously (41). In *b* a true double basement membrane is clearly evident (arrows) between the endothelium (*En*) and epithelium (*Ep*). Numerous coated pits and coated vesicles are present within the basal epithelial cytoplasm of a few broad foot processes (arrowheads). *CL*, capillary lumen. × 32,500.

endoplasmic reticulum and cytoplasmic vesicles of both endothelium and epithelium (Fig. 6*a*). When sections were incubated with control, laminin-adsorbed IgG–HRP (Fig. 6*b*) in contrast, peroxidase was completely absent from intracellular sites as well as basement membranes.

The double basement membranes seen in capillary loop stages were rarely seen in maturing glomeruli stages. These glomeruli contained several well-defined capillaries with an overall architecture closely similar to that of the adult. As seen before in adult glomeruli (1–3), peroxidase was present throughout the full thickness of the GBM but a new feature was found in peripheral capillary walls of the newborn that normally is absent in adults. Extensive loops or outpockets of additional basement membrane material appeared directly beneath differentiating epithelial foot processes and these segments were also completely labeled with anti-laminin IgG-HRP (Fig. 7). The outpockets were usually located in the epithelium surrounding the peripheral capillary loops and were rarely seen between cells overlying mesangial areas. In sections cut tangential to the capillary wall, peroxidase-positive basement membrane material extended far into the epithelial side of the wall but was always located between adjacent foot processes (Fig. 8). In contrast to the epithelium, no such outpockets of basement membrane were seen on the endothelial side of the capillary wall.

In lightly fixed sections of maturing glomeruli incubated in vitro with anti-laminin IgG-HRP, reaction product was localized within the GBM, outpockets, and rough endoplasmic reticulum of epithelial podocytes as seen in capillary loop stage glomeruli. Clear examples of intracellular staining in the endothelium were not obtained but these cells in maturing glomeruli had flattened themselves against the inner capillary wall and their cytoplasm was greatly attenuated. An inability to demonstrate intracellular staining in these cells may consequently have been due to the relatively small amount of endothelial cytoplasm exposed on section surfaces.

When normal, uninjected newborn rat kidneys that had been fixed and processed for standard electron microscopy were examined, numerous examples of additional basement membrane segments or outpockets on the epithelial side of

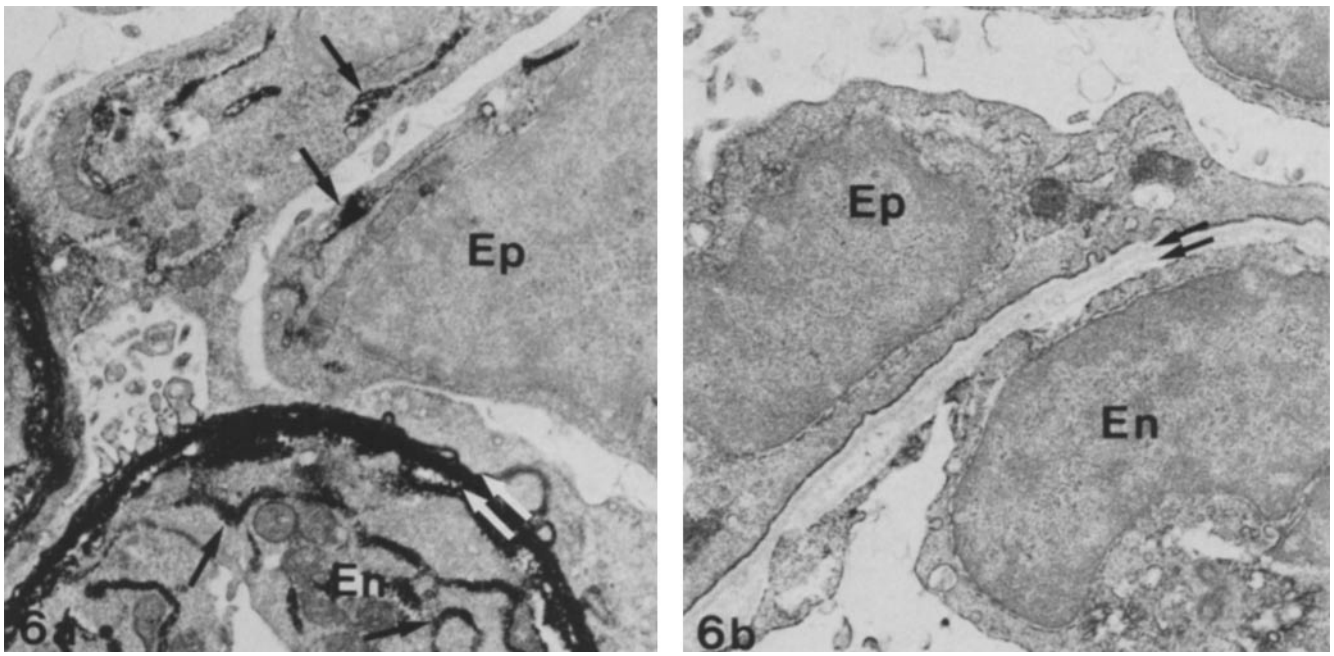

FIGURE 6 Electron micrographs of lightly fixed sections from newborn rat kidneys incubated in vitro with (*a*) anti-laminin IgG-HRP or (*b*) laminin-adsorbed IgG-HRP. Note that in *a* HRP is present within a double basement membrane (white arrows) and within cytoplasmic vesicles and rough endoplasmic reticulum (arrows) of the endothelium (*En*) and epithelium (*Ep*). (*b*) In contrast to *a*, *b* shows no staining of the double basement membrane (arrows) or intracellular structures within the endothelium (*En*) or epithelium (*Ep*) by laminin-adsorbed IgG-HRP. (*a*) × 19,150; (*b*) × 17,500.

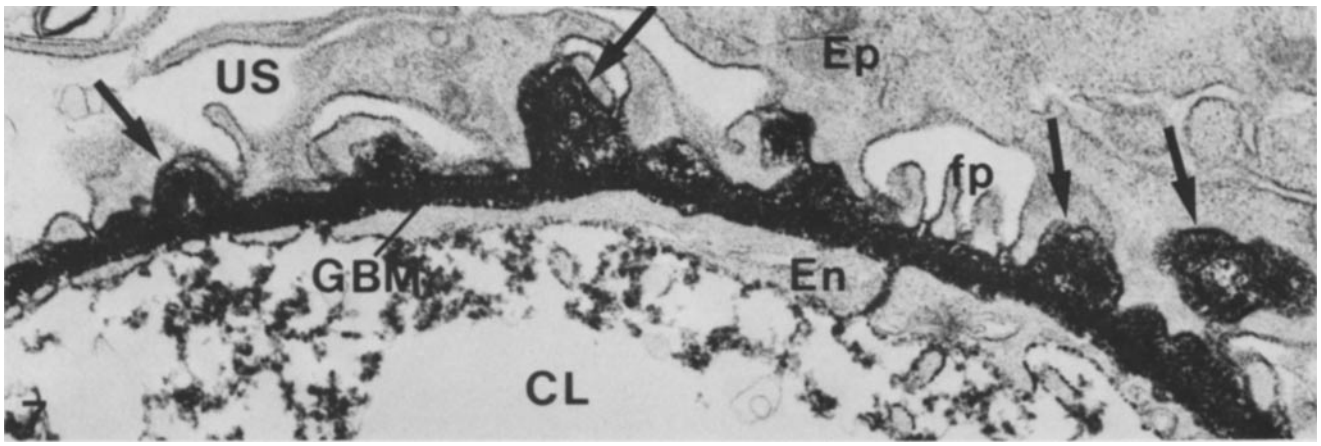

FIGURE 7 Glomerular capillary wall in a maturing glomerulus from a newborn rat that received anti-laminin IgG-HRP 1 h before fixation. HRP reaction product is present throughout the full thickness of the GBM. In addition, several loops or outpockets of peroxidase-positive basement membrane-like material are present on the epithelial (*Ep*) side of the capillary wall (arrows) beneath differentiating foot processes. A few apparently mature foot processes (*fp*) are also present. *CL*, capillary lumen; *En*, endothelium; *US*, urinary space. × 27,500.

the GBM could readily be located within maturing glomeruli (Fig. 9). This material had the same amorphous, finely granular ultrastructure as the GBM.

As is the case with adult rats (1–3), injected laminin-adsorbed IgG-HRP did not bind to newborn rat kidney basement membranes.

Pulse–Chase–Fix Studies of Developing GBMs

In contrast to the pulse–fix studies described above, the basement membrane distribution of HRP in pulse–chase–fix experiments was nonuniform. When kidneys were fixed 2–6 d after anti-laminin IgG-HRP injection, developing GBMs in the vesicle, comma, and S-shaped stages of nephrons were usually completely unlabeled, indicating that these nephrons had developed subsequent to the injection. Areas of labeled GBM were seen, however, within maturing glomeruli located deeper in the cortex, but here the amount of label varied considerably. In different loops and within individual loops the concentration of reaction product ranged from virtually nil to intense (Fig. 9). There was also a variation in the distribution of HRP across the GBM in maturing glomeruli and this was seen most frequently in kidneys fixed 4–6 d after

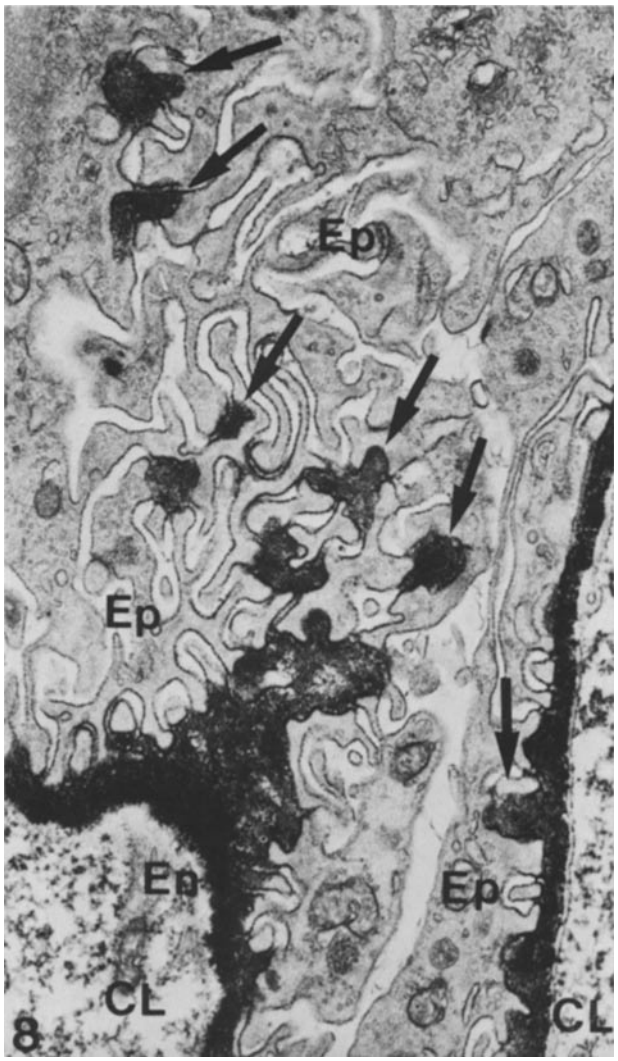

anti-laminin IgG-HRP injection (Figs. 10 and 11). When present within the GBM, HRP always occurred beneath the endothelium. Immediately overlying these stained areas of GBM, however, were unstained outpockets or loops of basement membrane material that lay beneath the differentiating epithelial foot processes (Figs. 10 and 11). Thus, the basement membrane segments on the epithelial side of the developing GBM that in pulse-fix experiments were completely labeled with anti-laminin IgG-HRP (Figs. 7 and 8) were often completely unlabeled in pulse-chase-fix studies (Figs. 10 and 11).

The segments of basement membrane on the epithelial side of glomerular capillary walls were not rare isolated findings but were observed within maturing glomeruli stages of all newborn rats examined by electron microscopy (Table I). To determine whether the injection of anti-laminin IgG-HRP influenced the incidence or distribution of these segments, a morphometric study was undertaken. Lengths of peripheral capillary loop GBM and lengths of the basement membrane outpockets on the epithelial side of capillary walls were measured from electron micrographs of normal, uninjected rat kidneys and then compared with those of pulse-fix and pulse-chase-fix rats. The outpockets averaged ~0.7 μm in length and occurred once every ~6.7 μm of linear glomerular capillary wall in all animals. Thus the injection of anti-laminin IgG neither affected the size range nor the incidence of the outpockets.

FIGURE 8 Glomerular capillary wall in a maturing glomerulus from a newborn rat that received anti-laminin IgG-HRP 1 h before fixation. On the right side of the figure the plane of section is perpendicular to a glomerular capillary wall and from the center to the left the section is cutting obliquely through an adjacent capillary. Anti-laminin-HRP is present throughout the GBM and is also observed within several segments of additional basement membrane that lie between differentiating epithelial (*Ep*) podocytes (arrows). *En*, endothelium; *CL*, capillary lumen. × 16,500.

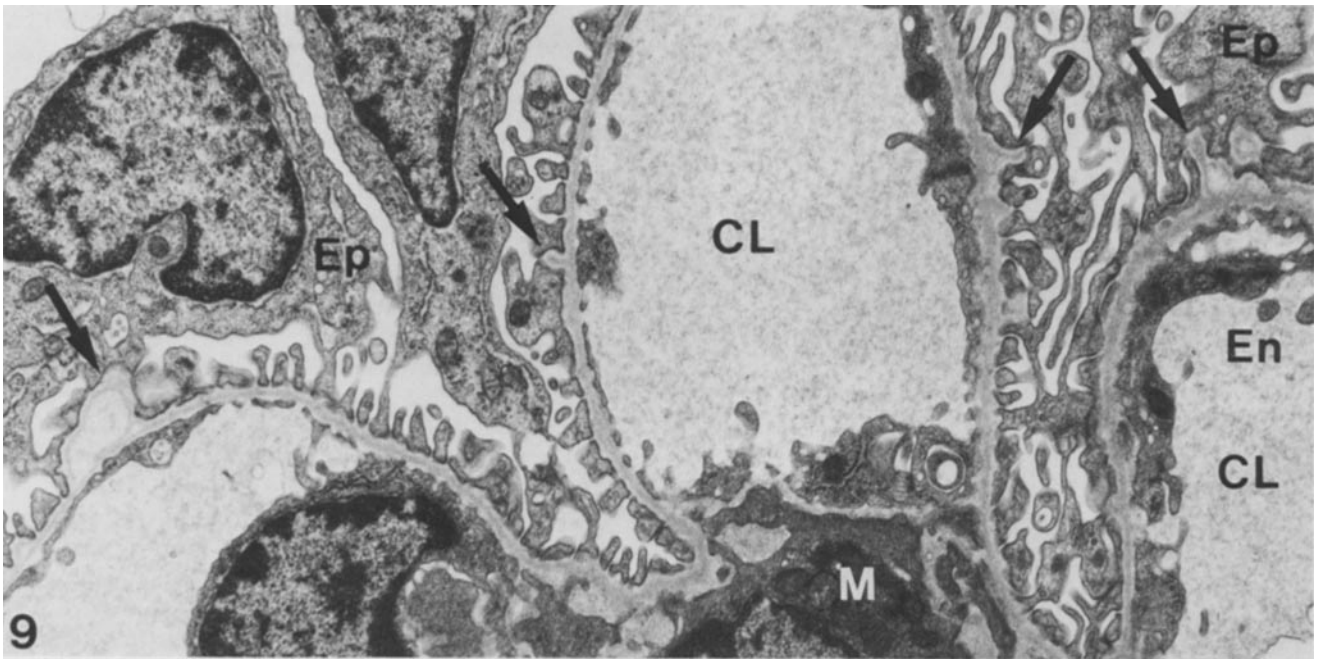

FIGURE 9 Portion of a maturing glomerulus from a normal, uninjected newborn rat processed for standard electron microscopy. Beneath the differentiating foot processes of the epithelium (*Ep*) are several examples of additional basement membrane outpockets (arrows). Note that such segments are seen only on the epithelial side of the capillary wall. *CL*, capillary lumen; *En*, endothelium; *M*, mesangium. × 10,900.

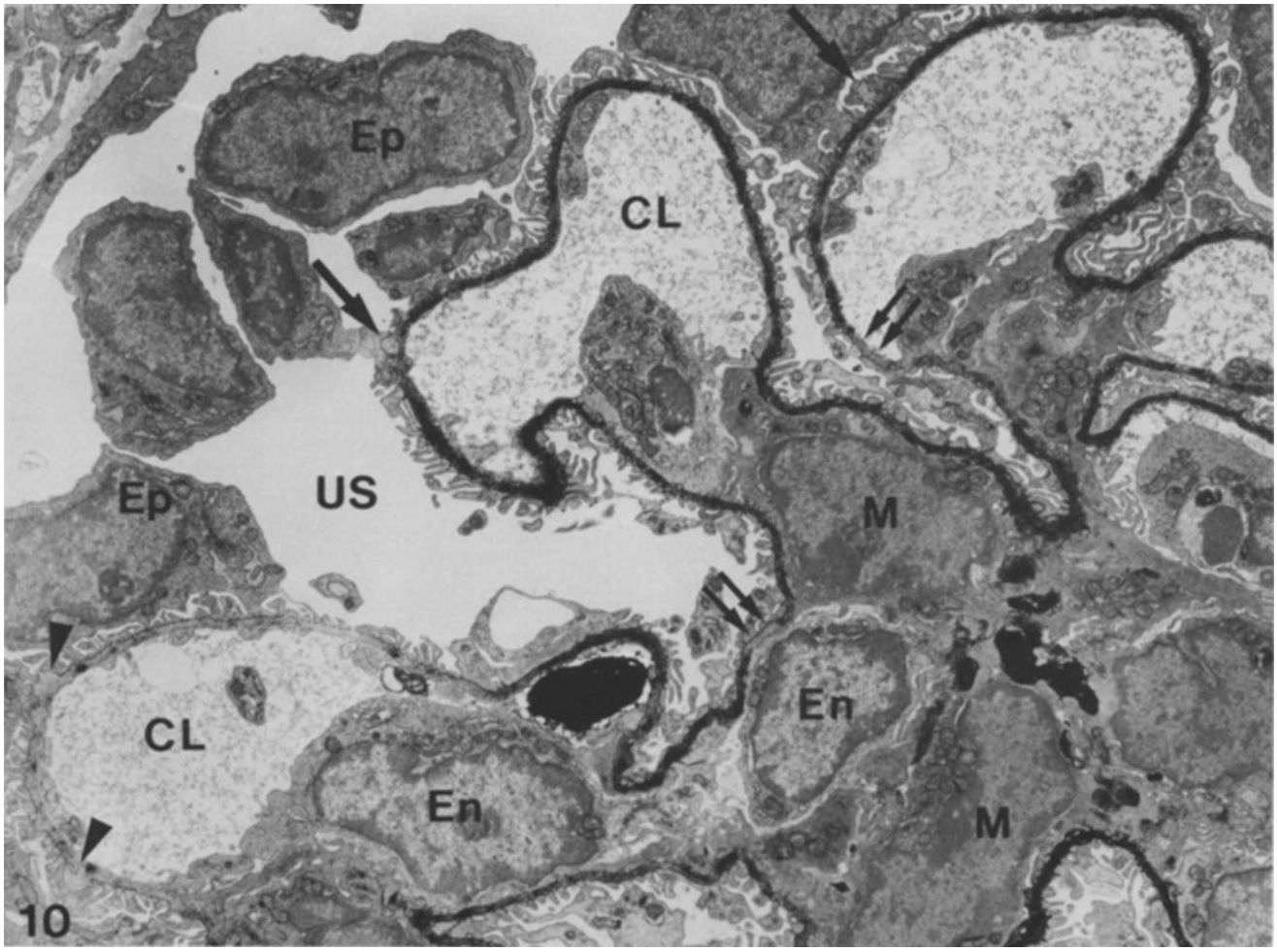

FIGURE 10 Portion of a maturing glomerulus from a pulse-chase-fix rat that received anti-laminin IgG-HRP on day 2 and was then fixed on day 6. In contrast to Fig. 4, note the uneven distribution of reaction product in the GBM of different capillary loops. Some segments of additional basement membrane material on the epithelial side of the capillaries appear unstained (single arrows). Sections of unstained GBM (double arrows) are also present. The capillary loop in the lower left corner is almost completely unstained and outpockets of basement membrane material appear to extend into the epithelium (arrowheads). *CL*, capillary lumen; *En*, endothelium; *M*, mesangium; *Ep*, epithelium; *US*, urinary space. × 5,800.

Pulse–Chase–Pulse Studies

Kidneys from rats that received intravenous injections of sheep anti-laminin IgG followed by biotin-rabbit anti-laminin IgG (Table I) were examined by double-label immunofluorescence microscopy. When the second injection came 7 or 8 d after the first, sheep anti-laminin was absent from the most cortical glomeruli but present in deeper glomeruli located in the juxtamedullary area (Fig. 12*a*). Similarly, sheep IgG was generally absent in tubular areas of the superficial cortex but present in the deeper cortex. Also in the deep cortex were circular unstained areas of tissue that were surrounded by fluorescing glomeruli and tubular basement membrane (TBM) (Fig. 12*a*). When the same section was examined by avidin-rhodamine, however, all glomeruli and TBMs throughout the entire section were stained (Fig. 12*b*). Unstained areas seen in Fig. 12*a* were now shown to contain glomeruli and tubules that undoubtedly had developed after the first injection had been given. In addition, the circular unstained areas seen in the deep cortex of Fig. 12*a* probably contained the loops of Henle from these newly developed nephrons (Fig. 12*b*). Variations in the binding pattern of anti-laminin to glomeruli at different levels in the cortex could also be demonstrated. In some peripheral glomeruli only the vascular stalk and what was probably the extraglomerular mesangium were stained with sheep anti-laminin IgG (Fig. 12*c*). Although the second injection with biotin-rabbit anti-laminin IgG left these structures largely unstained, the GBM in the rest of the glomerulus was stained intensely (Fig. 12*d*). This result suggests that the vascular stalks developed before the glomerular capillaries. In deep maturing glomeruli, sheep anti-laminin IgG was present most abundantly in mesangial regions but weak fluorescence was also usually seen throughout the GBM of peripheral capillary loops (Fig. 12*e*). The second injection, in contrast, resulted in complete, essentially uniform staining of GBM throughout maturing glomeruli (Fig. 12*f*).

DISCUSSION

The results from this study provide additional confirmatory evidence that the GBM develops from the fusion of endothelial and epithelial basement membranes before and during the capillary loop stage of glomerular development. After fusion, however, new basement membrane material, probably assembled solely by the epithelium, was inserted into existing GBM as glomeruli expanded and matured.

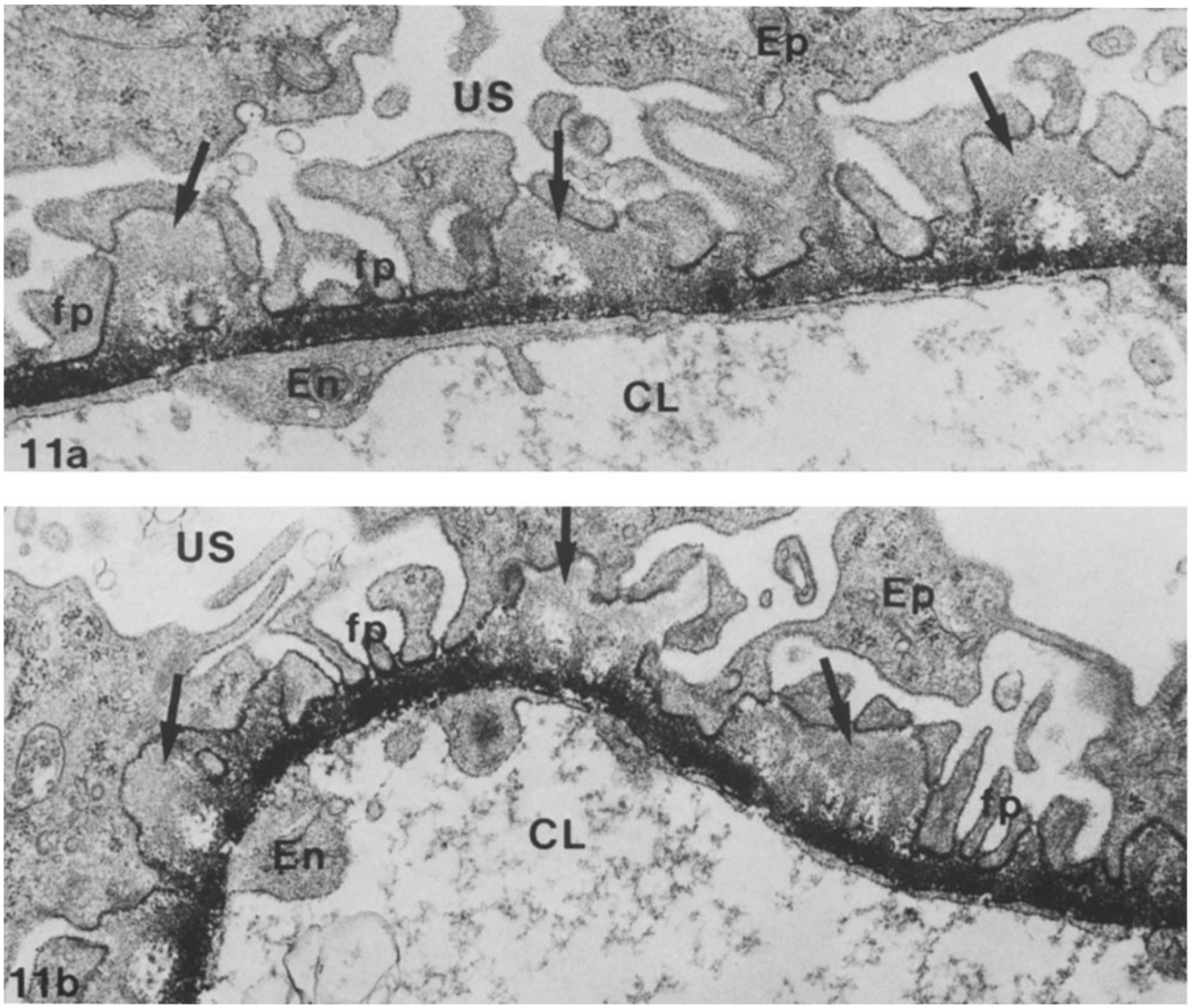

FIGURE 11 Higher magnification views of peripheral capillary wall in maturing glomeruli of pulse-chase-fix rats. HRP reaction product occurs immediately beneath the endothelium (*En*) and extends completely across the GBM to the epithelium (*Ep*) in areas where foot process (*fp*) formation appears complete. On the epithelial (*Ep*) side of the capillary wall, however, several loops or segments of unstained additional basement membrane material are also seen, and these usually occur beneath foot processes that are still apparently developing (arrows). Compare with Figs. 7 and 8. (*a*) × 39,000; (*b*) × 32,000.

Endothelial and Epithelial Basement Membrane Fusion

In S-shaped and developing capillary loop stages, anti-laminin IgG-HRP decorated a double layer of basement membrane between closely apposed endothelial and epithelial cells. Due to electron microscopic images of the intermingling of the two basement membranes and because such structures are rarely seen in glomeruli at later developmental stages, the concept that the two basement membranes fuse to give rise to the GBM has emerged (27, 42, 47, 50). Indeed, when GBM from adult glomeruli are treated with guanidine, two morphologically distinct layers are seen: an electron lucent endothelia lamina and an electron opaque epithelial lamina (21).

When anti-laminin IgG-HRP was applied to newborn rat kidney sections in vitro, reaction product was present within the rough endoplasmic reticulum of both endothelium and epithelium, indicating that both cell types participated in the deposition of laminin within the developing GBM. This immunoelectron microscopic result appears to confirm recent immunofluorescent experiments with quail/mouse hybrid glomeruli and species specific monoclonal and polyclonal anti-type IV collagen antibodies that show the hybrid GBM contains collagen derived from both endothelium and epithelium (46).

The biochemical events governing basement membrane fusion are unknown, but perhaps interactions between some of the macromolecules contained within the dual basement membrane knit the two structures together. Consistent with such a possibility, type IV collagen, laminin, and heparan sulfate proteoglycans all share affinities for one another in vitro (19, 30, 45, 52). The functional significance of basement membrane fusion is also unknown, but the fusion may (*a*) cement the spatial relationship between the developing endothelium and overlying epithelium and (*b*) provide a denser, more effective barrier to the passage of plasma proteins.

In addition to basement membranes of capillary loop stage nephrons, HRP reaction product was also seen within proxi-

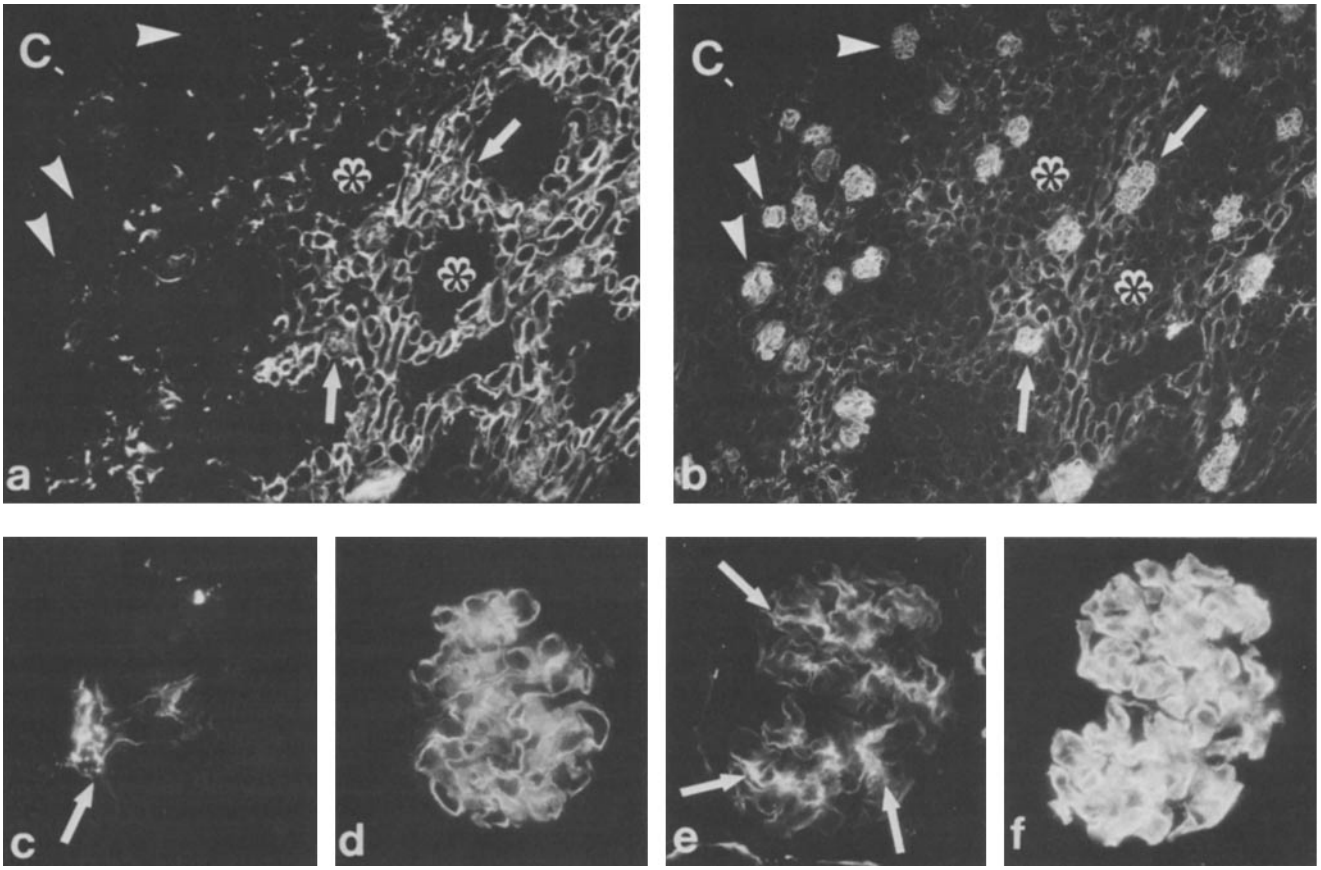

FIGURE 12 Paired immunofluorescence micrographs of cryostat sections of kidneys from newborn rats injected with sheep anti-laminin IgG on day 2 and then re-injected 7 d later with biotin-rabbit anti-laminin IgG (pulse–chase–pulse). Kidneys were removed 1 h after the second injection. Sections were doubly stained with fluorescein-anti-sheep IgG (to detect antibody bound after the first injection) and rhodamine-avidin (to detect antibody from the second injection). *a, c,* and *e* show the distribution of fluorescein and *b, d,* and *f* show the distribution of rhodamine. (*a*) Renal cortex. Sheep anti-laminin IgG is present within glomeruli (arrows) and TBM in the juxtamedullary area. Note circular unstained regions (*). Superficial glomeruli (arrowheads) can barely be detected immediately beneath the capsule (*C*) but these are not labeled. (*b*) In contrast to *a*, *b* shows that glomeruli (arrowheads) and TBM throughout the entire cortex are stained. TBM fluorescence (*) is also seen in areas that were unstained in *a*. *C*, capsule. (*c*) Superficial glomerulus. Sheep anti-laminin is present only near the vascular pole (arrow). (*d*) In contrast to *c*, *d* shows that GBM within peripheral capillary loops fluoresce intensely whereas little fluorescence is seen at the vascular pole. (*e*) Glomerulus near the juxtamedullary zone. Weak fluorescence is present throughout the GBM but is more intense in mesangial areas (arrows). (*f*) Upon re-injection of anti-laminin IgG, basement membranes throughout the glomerulus fluoresce with the same apparent intensity. (*a* and *b*) × 100. *c–f*) × 250.

mal tubular epithelium in endocytic vesicles and within dense bodies corresponding to lysosomes. In contrast, after the injection of anti-laminin IgG-HRP into healthy adult rats, HRP is not seen in the tubular epithelium (1–3). Although large circulating proteins may therefore cross the glomerular filter during capillary loop development, most of these may subsequently be recovered by the proximal tubule because proteinuria is generally not observed during fetal and neonatal stages (13).

Addition of New Basement Membrane by the Epithelium

A new finding in this study was the identification in maturing glomeruli of irregular segments or outpockets of basement membrane-like material extending far into the epithelial side of the capillary wall between developing podocytes. In kidneys that were fixed 1 h after anti-laminin IgG-HRP injection, peroxidase was always present throughout the full dimensions of the segments. The likelihood that HRP reaction could nonspecifically diffuse (12) with such uniformity throughout these large structures seems remote. In addition, the outpockets were not artifactually induced by anti-laminin IgG, because they were localized with the same frequency in uninjected newborns.

In kidneys that were fixed several days after the injection of anti-laminin IgG-HRP, however, the basement membrane outpockets seen on the epithelial side of capillary walls were often completely unlabeled. In contrast, HRP reaction product was frequently present within lengths of GBM immediately beneath the unlabeled segments. This observation strongly suggests that the unlabeled segments arose exclusively from the glomerular epithelium at some point in time after anti-laminin IgG-HRP injection. Results from the pulse–chase–pulse experiments further support the observation that basement membrane deposition continued during glomerular maturation. Whereas IgG from the first injection was weakly present in capillary loop GBM of maturing glomeruli, IgG from the second injection intensely stained these same sites. Although this report documents basement membrane assembly apparently conducted exclusively by the glomerular epithelium in vivo, several earlier studies have demonstrated the

ability of cultured glomerular epithelium to synthesize basement membranes or components in vitro (4, 6, 8, 29). The endothelium may also contribute to GBM formation in maturing glomeruli, but segments of basement membrane as seen on the epithelial side of the capillary wall were never observed in the endothelial layer.

Two Stages in GBM Development

Taken together, these results indicate that GBM assembly occurs by at least two different processes during glomerular development. First, during early stages, endothelial and epithelial basement membranes fuse. After fusion, GBM assembly continues in maturing glomeruli where capillaries blossom and podocytes undergo extensive foot process formation. As foot processes from neighboring cells interdigitate, sections of new basement membrane may simultaneously be assembled by the epithelium and inserted into the fused basement membrane. The result would thus be an expansion of the capillary wall and filtration surface area.

Once the glomerulus and the GBM have attained their mature configurations, double basement membranes and extensive outpockets into the epithelium are not seen, but GBM remodeling probably continues during the process of aging. GBM proteoglycan turnover has been estimated to have a half-life of ~7 d (11), whereas turnover for GBM collagen is believed to be much slower, with a half-life of >100 d (40). Long-term labeling studies in mature rats concluded that GBM components are continuously synthesized exclusively by the epithelia (31), or jointly by the endothelia and epithelia (51), and slowly translocated into mesangial regions for degradation (51). In agreement with this proposed turnover pathway, GBM-bound anti-laminin IgG appears to be gradually cleared from the peripheral GBM over a period of several months and concentrated within the mesangium (1).

I thank Mrs. Elizabeth W. Perry for expert technical assistance and photography, Dr. Richard Mayne for type IV collagen used in the inhibition enzyme-linked immunosorbent assay, and Ms. Maxine Humphrey for word processing.

These experiments were funded by grants from the American Heart Association, Alabama Affiliate, Inc., and the National Institutes of Health (AM 34972).

Animals used in this study were maintained in accordance with policies established by veterinarians at the University of Alabama at Birmingham, and with those of the National Institutes of Health.

Received for publication 14 December 1984, and in revised form 25 February 1985.

REFERENCES

1. Abrahamson, D. R., and J. P. Caulfield. 1982. Proteinuria and structural alterations in rat glomerular basement membranes induced by intravenously injected anti-laminin immunoglobulin G. *J. Exp. Med.* 156:128–145.
2. Abrahamson, D. R., A. Hein, and J. P. Caulfield. 1983. Laminin in glomerular basement membranes of aminonucleoside nephrotic rats. Increased proteinuria induced by anti-laminin immunoglobulin G. *Lab. Invest.* 49:38–47.
3. Abrahamson, D. R., and J. P. Caulfield. 1985. Distribution of laminin within rat and mouse renal, splenic, intestinal, and hepatic basement membranes identified after the intravenous injection of heterologous anti-laminin IgG. *Lab. Invest.* 52:169–181.
4. Avner, E. D., R. Jaffe, T. Temple, D. Ellis, and A. E. Chung. 1983. Development of renal basement membrane glycoproteins in metanephric organ culture. *Lab. Invest.* 48:263–268.
5. Bayer, E. A., M. Wilchek, and E. Skutelsky. 1976. Affinity cytochemistry: The localization of lectin antibody receptors on erythrocytes via the avidin-biotin complex. *FEBS (Fed. Eur. Biochem. Soc.) Lett.* 68:240–244.
6. Bernstein, J., F. Cheng, and J. Roszka. 1981. Glomerular differentiation in metanephric organ culture. *Lab. Invest.* 45:183–190.
7. Bitter, T., and H. M. Muir. 1962. A modified uronic acid carbazole reaction. *Anal. Biochem.* 4:330–334.
8. Bonadio, J. F., H. Sage, F. Cheng, J. Bernstein, and G. E. Striker. 1984. Localization of collagen types IV and V, laminin, and heparan sulfate proteoglycan to the basal lamina of kidney epithelial cells in transfilter metanephric culture. *Am. J. Pathol.* 116:289–296.
9. Carlin, B., R. Jaffe, B. Bender, and A. E. Chung. 1981. Entactin, a novel basal lamina-associated sulfated glycoprotein. *J. Biol. Chem.* 256:5209–5214.
10. Caulfield, J. P., and M. G. Farquhar. 1974. The permeability of glomerular capillaries to graded dextrans. Identification of the basement membrane as the primary filtration barrier. *J. Cell Biol.* 63:883–903.
11. Cohen, M. P., and M. L. Surma. 1982. In vivo biosynthesis and turnover of ^{35}S-labeled glomerular basement membrane. *Biochem. Biophys. Acta.* 716:337–340.
12. Courtoy, P. J., D. H. Picton, and M. G. Farquhar. 1983. Resolution and limitations of the immunoperoxidase procedure in the localization of extracellular matrix antigens. *J. Histochem. Cytochem.* 31:945–951.
13. DuBois, A. M. 1969. The embryonic kidney. *In* The Kidney: Morphology, Biochemistry, and Physiology. Vol. 1. C. Rouiller and A. F. Muller, editors. Academic Press, Inc., New York. 1–60.
14. Ekblom, P., K. Alitalo, A. Vaheri, R. Timpl, and L. Saxen. 1980. Induction of a basement membrane glycoprotein in embryonic kidney: possible role of laminin in morphogenesis. *Proc. Natl. Acad. Sci. USA.* 77:485–489.
15. Ekblom, P. 1981. Formation of basement membranes in the embryonic kidney: an immunohistological study. *J. Cell Biol.* 91:1–10.
16. Ekblom, P. 1981. Determination and differentiation of the nephron. *Med. Biol.* 59:139–160.
17. Farquhar, M. G., and G. E. Palade. 1965. Cell junctions in amphibian skin. *J. Cell Biol.* 26:263–291.
18. Farquhar, M. G. 1981. The glomerular basement membrane: a selective macromolecular filter. *In* Cell Biology of Extracellular Matrix. E. D. Hay, editor. Plenum Publishing Corp., New York. 335–378.
19. Fujiwara, S., H. Wiedemann, R. Timpl, A. Lustig, and J. Engel. 1984. Structure and interactions of heparan sulfate proteoglycans from a mouse tumor basement membrane. *Eur. J. Biochem.* 143:145–157.
20. Graham, R. C., and M. J. Karnovsky. 1966. The early stages of absorption of injected horseradish peroxidase in the proximal tubules of mouse kidney. Ultrastructural cytochemistry by a new technique. *J. Histochem. Cytochem.* 14:291–302.
21. Huang, T. W. 1979. Basal lamina heterogeneity in the glomerular capillary tufts of human kidneys. *J. Exp. Med.* 149:1450–1459.
22. Jokelainen, P. 1963. An electron microscope study of the early development of the rat metanephric nephron. *Acta Anat.* 52(Suppl. 47):1–71.
23. Kanwar, Y. S., and M. G. Farquhar. 1979. Anionic sites in the glomerular basement membrane. In vivo and in vitro localization to the laminae rarae by cationic probes. *J. Cell Biol.* 81:137–153.
24. Kanwar, Y. S., and M. G. Farquhar. 1979. Presence of heparan sulfate in the glomerular basement membrane. *Proc. Natl. Acad. Sci. USA.* 76:1303–1307.
25. Karnovsky, M. J. 1965. A formaldehyde-glutaraldehyde fixative of high osmolality for use in electron microscopy. *J. Cell Biol.* 27 (No. 2, Pt. 2):137*a*. (Abstr.)
26. Karnovsky, M. J. 1979. The structural basis for glomerular filtration. *In* Kidney Disease: Present Status. J. Churg, B. H. Spargo, F. K. Mostofi, M. R. Abell, editors. Williams & Wilkins Co., Baltimore. 1–41.
27. Kazimierczak, J. 1971. Development of the renal corpuscle and the juxtaglomerular apparatus. A light and electron microscopic study. *Acta Pathol. Microbiol. Scand. Sect. A Suppl.* 218:1–61.
28. Kefalides, N. A. 1979. Biochemistry and metabolism of basement membranes. *Int. Rev. Cytol.* 61:167–228.
29. Killen, P. D., and G. E. Striker. 1979. Human glomerular visceral epithelial cells synthesize a basal lamina collagen in vitro. *Proc. Natl. Acad. Sci. USA.* 76:3518–3522.
30. Kleinman, H. K., M. L. McGarvey, J. R. Hassell, and G. R. Martin. 1983. Formation of a supramolecular complex is involved in the reconstitution of basement membrane components. *Biochemistry.* 22:4969–4974.
31. Kurtz, S. M., and J. D. Feldman. 1962. Experimental studies on the formation of the glomerular basement membrane. *J. Ultrastruct. Res.* 6:19–27.
32. Laurie, G. W., C. P. Leblond, and G. R. Martin. 1982. Localization of type IV collagen, laminin, heparan sulfate proteoglycan, and fibronectin to the basal lamina of basement membranes. *J. Cell Biol.* 95:340–344.
33. Laurie, G. W., C. P. Leblond, S. Inoue, G. R. Martin, and A. E. Chung. 1984. Fine structure of the glomerular basement membrane and immunolocalization of five basement membrane components to the lamina densa (basal lamina) and its extensions in both glomeruli and tubules of the rat kidney. *Am. J. Anat.* 169:463–481.
34. Lemkin, M. C., and M. G. Farquhar. 1981. Sulfated and nonsulfated glycosaminoglycans and glycopeptides are synthesized by kidney *in vivo* and incorporated into glomerular basement membranes. *Proc. Natl. Acad. Sci. USA.* 78:1726–1730.
35. Martinez-Hernandez, A., S. Gay, and E. J. Miller. 1982. Ultrastructural localization of type V collagen in rat kidney. *J. Cell Biol.* 92:343–349.
36. Martinez-Hernandez, A., E. J. Miller, I. Damjanov, and S. Gay. 1982. Laminin-secreting yolk sac carcinoma of the rat. Biochemical and electron immunohistochemical studies. *Lab. Invest.* 47:247–257.
37. Martinez-Hernandez, A., and A. E. Chung. 1984. The ultrastructural localization of two basement membrane components: entactin and laminin in rat tissues. *J. Histochem. Cytochem.* 32:289–298.
38. Monaghan, P., M. J. Warburton, N. Perusinghe, and P. S. Rudland. 1983. Topographical arrangement of basement membrane proteins in lactating rat mammary gland: comparison of the distribution of type IV collagen, laminin, fibronectin, and Thy-1 at the ultrastructural level. *Proc. Natl. Acad. Sci. USA.* 80:3344–3348.
39. Nakane, P. K., and A. Kawaoi. 1974. Peroxidase-labeled antibody. A new method of conjugation. *J. Histochem. Cytochem.* 22:1084–1091.
40. Price, R. G., and R. G. Spiro. 1977. Studies on the metabolism of the renal glomerular basement membrane. *J. Biol. Chem.* 252:8597–8602.
41. Reeves, W., J. P. Caulfield, and M. G. Farquhar. 1978. Differentiation of epithelial foot processes and filtration slits. Sequential appearance of occluding junctions, epithelial polyanion, and slit membranes in developing glomeruli. *Lab. Invest.* 39:90–100.
42. Reeves, W. H., Y. S. Kanwar, and M. G. Farquhar. 1980. Assembly of the glomerular filtration surface. Differentiation of anionic sites in glomerular capillaries of newborn rat kidney. *J. Cell Biol.* 85:735–753.
43. Reynolds, E. S. 1963. The use of lead citrate at high pH as an electron-opaque stain in electron microscopy. *J. Cell Biol.* 17:208–212.
44. Rodewald, R. 1980. Distribution of immunoglobulin G receptors in the small intestine of the young rat. *J. Cell Biol.* 85:18–32.
45. Sakashita, S., E. Engvall, and E. Ruoslahti. 1980. Basement membrane glycoprotein laminin binds to heparin. *FEBS (Fed. Eur. Biochem. Soc.) Lett.* 116:243–246.

46. Sariola, H., R. Timpl, K. von der Mark, R. Mayne, J. M. Fitch, T. F. Linsenmayer, and P. Ekblom. 1984. Dual origin of glomerular basement membrane. *Dev. Biol.* 101:86–96.
47. Thorning, D., and R. Vracko. 1977. Renal glomerular basal lamina scaffold. Embryological development, anatomy, and role in cellular reconstruction of rat glomeruli injured by freezing and thawing. *Lab. Invest.* 37:105–119.
48. Timpl, R., H. Rohde, P. G. Robey, S. I. Rennard, J.-M. Foidart, and G. R. Martin. 1979. Laminin—a glycoprotein from basement membranes. *J. Biol. Chem.* 254:9933–9937.
49. Timpl, R., M. Dziadek, S. Fujiwara, H. Nowack, and G. Wick. 1983. Nidogen: a new, self-aggregating basement membrane protein. *Eur. J. Biochem.* 137:455–465.
50. Vernier, R. L., and A. Birch-Andersen. 1962. Studies of the human fetal kidney. I. Development of the glomerulus. *J. Pediatr.* 60:754–767.
51. Walker, F. 1973. The origin, turnover and removal of glomerular basement membrane. *J. Pathol.* 110:233–244.
52. Woodley, D. T., C. N. Rao, J. R. Hassell, L. A. Liotta, G. R. Martin, and H. K. Kleinman. 1983. Interactions of basement membrane components. *Biochem. Biophys. Acta.* 761:278–283.